Interactions at the Silica-Peptide Interface: Influence of the Extent of Functionalization on the Conformational Ensemble

*Anna Sola-Rabada,†[a] Monika Michaelis,[§,†a] Daniel J Oliver,† Martin J. Roe,[‡] Lucio Colombi Ciacchi[§,+] Hendrik Heinz[ϕ] and Carole C. Perry[†]**

†Biomolecular and Materials Interface Research Group, Interdisciplinary Biomedical Research Centre, School of Science and Technology, Nottingham Trent University, Clifton Lane, Nottingham NG11 8NS, United Kingdom.

§Hybrid Materials Interfaces Group, Bremen Center for Computational Materials Science (BCCMS) and Center for Environmental Research and Sustainable Technology (UFT), Faculty of Production Engineering, University of Bremen, 28359 Bremen, Germany.

‡Advanced Materials Research Group, X-ray Photoelectron Spectroscopy, Faculty of Engineering, The University of Nottingham, University Park, Nottingham, NG7 2RD, UK.

[+]MAPEX Center for Materials and Processes, University of Bremen, 28359 Bremen, Germany

[ϕ]Department of Chemical and Biological Engineering, University of Colorado at Boulder, Boulder, CO 80309, USA

[a]These two authors contributed equally

KEYWORDS Silica, peptide, interactions, methyl groups, amine groups, level of functionalization, adsorption isotherms, interaction switch, circular dichroism spectroscopy.

ABSTRACT In this contribution, the effect of silica particle size (28 and 210 nm) and surface chemistry (i.e. hydroxyl, methyl or amino groups) on peptide binding response is studied with a

specific emphasis on the effect of extent of functionalization on binding. Exhaustive characterization of the silica surfaces was crucial for knowledge of the chemistry and topography of the solid surface under study; and thus, to understand their impact on adsorption and the conformational ensemble of the peptides. The extent of surface functionalization was shown to be particle-size dependent, a higher level of 3-aminopropyl functionality being obtained for smaller particles, while a higher degree of methyl group functionality was found on the larger particles. We demonstrated that peptide interactions at the aqueous interface were not only influenced by the surface chemistry but by the extent of functionalization where a 'switch' of peptide adsorption behavior was observed, while changes in the conformational ensemble revealed by circular dichroism were independent of the extent of functionalization. In addition to electrostatic interactions and hydrogen bonding driving interaction at the silica-peptide interface the data obtained suggested that stronger interactions such as hydrophobic and/or covalent interactions may moderate interaction. The insights gained from this peptide-mineral study give a more comprehensive view of mechanisms concerning mineral-peptide interactions which may allow for the design and synthesis of novel (nano)materials with properties tailored for specific applications.

Introduction

Synthetic NPs have received much attention in recent years for a variety of technological and biomedical applications. The unique properties of NPs to some extent lie in their reduced size that confers on them high specific surface area. Therefore, NPs present a greater fraction of surface atoms and increased surface energy affecting both their chemical and physical properties.[1] The use of NPs in drug delivery systems is attractive due to their relatively large surface and permeability through many pathways across membranes resulting in high interaction with biological systems.[2] Taking the concept further, organic/inorganic nanocomposite materials have been developed as they combine advantages of both the inorganic material (i.e. rigidity, thermal stability) and the organic polymer (i.e. flexibility, dielectric, ductility, and processability). [2] Amorphous silica nanoparticles (SiNPs) have been extensively used due to their low-toxicity, easy surface modification and remarkable colloidal stability in physiological fluids.[3] Immobilization of organic polymers (i.e. proteins, DNA, and enzymes) or dyes onto functionalized surface SiNPs have been investigated since this has the potential to enhance and/or control interactions between the NPs and the molecule of interest.[2-4] However, the effects of functional groups on the surface properties of SiNPs, and further, the mechanisms concerning nanoparticle-biomolecule interactions are not fully understood. Thus, a specific emphasis and novel aspect of the present study was to explore the effect of surface functionalization on binding of biomolecules such as peptides. Amino- and methyl-functionalized silica particles were used since this allowed the effect of (positive) electrostatic interactions and hydrophobic interactions to be investigated. The ability to generate enhanced cell compatibility opens up the possibility to bind molecules that could be used for drug delivery (i.e. peptides, ligand).[5]

Previous studies in our group using phage display have identified 7-mer peptides of different overall charge that bind to silica.[6,7] For these peptides we have shown that the mechanisms of interaction include electrostatic, hydrogen-bonding and van der Waals interaction.[6,7] We have also demonstrated that particle size and surface modification influence the mineral-peptide binding response.[8] Further, and perhaps remarkably, it was observed that a greater extent of interaction occurred with increased particle size independent of the properties of these peptides.[8] Experimental data, supported by computational studies showed that peptides were anchored to the silica surface in a size dependent manner (i.e. 210 nm > 82 nm > 28 nm).[9] Further, the peptide binding mechanism for larger particles was dominated by electrostatic interactions.[9] For the current studies, the same peptide sequences KLPGWSG (K7), AFILPTG (A7) and LDHSLHS (L7) were selected essentially for their affinity to the silica surface and their difference in net charge (positive, neutral and negative) at the working pH. Circular dichroism spectroscopy was used to elucidate changes of the conformational ensemble of these peptides upon adsorption on nanoparticles with different chemical identity (-OH, $-CH_3$, $-NH_3^+$) at different levels of functionalization.

Since nanodelivery systems are designed to have drugs absorbed onto the particle surface, the level of functionalization of the SiNPs has been investigated as it may affect the amount of biomolecules absorbed and/or mechanisms of interaction. Thus, the specific aims of this study are to (i) achieve different levels of functionalization on different sized SiNPs, (ii) investigate the extent of functionalization on peptide binding, and (iii) determine if peptide conformation changes upon adsorption.

Materials and Methods

Materials. For the silica synthesis and functionalization, tetraethyl orthosilicate (TEOS, 98%, reagent grade), aminopropyltriethoxysilane (APTES, 99%) and tetramethyl orthosilicate (MTEOS, 98%) were purchased from Sigma-Aldrich; ammonia solution (NH_3, 35%) and acetic acid (CH_3COOH, > 99%) from Fisher Scientific and ethanol (EtOH, anhydrous, ≥ 99.5%) from Hayman Ltd. For the back titration of the ammonia stock solution prepared, 1 M HCl and 1 M KOH volumetric standard from Sigma-Aldrich were used. For peptide synthesis and characterization, piperazine ($C_4H_{10}N_2$), ,N'-Diisopropylethylamine (DIPEA, $C_8H_{19}N$), trifluoroacetic acid (TFA, $C_2HF_3O_2$), thioanisole (C_7H_8S), 3,6-Dioxa-1,8-octanedithiol (DODT, $C_6H_{14}O_2S_2$) were purchased from Sigma-Aldrich; N,N-dimethylformamide (DMF), dichloromethane (DCM), N-methyl-2-pyrrolidinone (NMP), and diethyl ether were purchased from Fisher Scientific; O-Benzotriazole-N,N,N',N'-tetramethyl-uronium-hexafluor-phosphate (HBTU) and all Fmoc-protected amino acids required for peptide synthesis and the preloaded-TGT resins were obtained from Novabiochem®. Sample preparation for HPLC and Mass Spectrometry employed acetonitrile (ACN) and TFA, both purchased from Sigma-Aldrich. For binding studies, solutions were prepared with phosphate buffered saline (PBS) tablets from Fisher Scientific in distilled-deionized water (ddH_2O) with conductivity less than 1 $\mu S \cdot cm^{-1}$. For CD studies, synthetic peptides K7, A7 and L7 with purity >95% were purchased from JPT (Germany).

Silica Synthesis. The growth of nanoscale silica particles was carried out using a modified Stöber synthesis method.[10] Following this method, TEOS and ammonia were chosen as the silica precursor and base, respectively. Both solutions (TEOS and ammonia) were separately prepared. Firstly, 22.3 ml of TEOS solution (98%, reagent grade) was diluted with 76.6 ml of ethanol. Secondly, 21.3 ml of NH_3 stock solution was diluted with 80 ml of ethanol. In this study, concentrations of ammonia in a range 0.25 - 10 M were used to achieve the desired particle sizes,

from 28 to 210 nm. For accurate preparation of the ammonia stock solutions, the concentration was determined prior to each experiment by back titrating a mixture of 1 M NH_3 and HCl with a 1 M KOH volumetric standard. Freshly made samples (TEOS and ammonia) were heated in a water bath at 50 °C for 1 hour prior to the addition of the TEOS solution into the ammonia solution. The mixtures were vigorously stirred and placed again in the water bath at 50 °C for up to 24 hours. Collected samples were centrifuged at 10000 rpm for 10 minutes to separate any precipitate from the supernatant. The supernatant was carefully separated by the aid of a Pasteur pipette and only ~80% of the supernatant was drawn from the vial although no precipitates were visible at the bottom of the vial (this was the case for particle sizes < 100 nm). The precipitates were re-dissolved in ethanol and re-centrifuged using the same conditions as above and, finally, washed three times with ddH_2O. For each washing, the samples were centrifuged at 5000 rpm for 5 minutes. Cleaned precipitates were lyophilized at -70°C using a Virtis-110 freeze-dryer.

Silica Functionalization. The grafting (post-modification) of the silica particles with aminopropyl (-$(CH_2)_3$-NH_2) and methyl (-CH_3) groups, hereafter named NH_2-$(CH_2)_3$-SiO_2 and CH_3-SiO_2 respectively, was performed using MTEOS and APTES solutions. Different levels of functionalization were achieved by increasing the concentrations of APTES and MTEOS (from 10 to 500 mM) until saturation was reached. The chosen concentrations of APTES and MTEOS were added to solutions containing the silica particles, stirred vigorously for 10 seconds and the reaction allowed to continue for a further 24 hours at room temperature under moderate stirring.

Characterization of SiNPs. The morphology and size of selected precipitates were studied using SEM (JEOL JSM-840A, 20 kV) and TEM (JEOL 2010, 200 kV). For SEM analysis, samples were attached using double-sided carbon adhesive tape to SEM stubs and carbon coated (Edwards, sputter coater S150B). For TEM analysis, samples were dispersed in ethanol prior to addition onto

the copper grids and analyzed after solvent evaporation was complete. Silica particle size (diameter) was determined from an average of more than 50 particles from SEM and TEM images using Java-based image processing program (*ImageJ* software). DLS (Zetasizer Nano S) was also employed for particle size analysis (silica particles in 5% EtOH solution) and for zeta potential determination of silica samples (silica particles in PBS solution, pH = 7.4). ATR (Perkin Elmer Spectrum 100 Series Spectrometer with Diamond/KRS-5 crystal) was used to detect the functional groups present in the lyophilized precipitates. Spectra were averaged from 32 scans at 4 cm^{-1} resolution with air as background. The organic content in the samples was determined by thermogravimetric analysis, TGA (Mettler Toledo TGA/SDTA 851^e) where samples were heated at 10 ° min^{-1} from 30 °C to 900 °C in air to ensure complete combustion of all organic material. All samples were analysed in duplicate as a minimum. The sample surface area and the N_2 adsorption-desorption isotherms were obtained on approximately 100 mg of sample powder by Gas adsorption analysis (Quantochrome Nova 3200e). Samples were degassed at 100 °C overnight prior to each analysis. The surface area was determined by the Brunauer–Emmett–Teller (BET) method[11] using a five-point adsorption isotherm in the relative pressure range of P/P_0 = 0.05/0.3 at 77.35 K. Sample porosity (pore size distribution) was obtained by the Barrett-Joyner-Halenda (BJH) method[12] from the desorption branch of the isotherm. The chemical constitution of the precipitates was investigated by XPS using a VG Scientific ESCALab MkII X-ray photoelectron spectrometer with an Al Kα X–ray source (hν = 1486.6 eV). Samples were ground and then mounted on standard sample holders. Before analysis, the calibration and linearity of the binding energy scale was checked with a pure silver sample using the peak positions of the $Ag3d_{5/2}$ photoelectron line (at 368.26 eV) and the AgM_4NN Auger line (at 1128.78 eV). Survey spectra of precipitates were collected covering the full BE range from 0 - 1200 eV using a step size of 1 eV,

a dwell time of 0.2 seconds and PE of 50 eV. High resolution core level spectra of the Si 2p, C 1s, O 1s and N 1s peaks were collected using a PE of 20 eV, a step size of 0.2 and a dwell time of 0.4 seconds, which were subsequently deconvoluted and fitted using standard mixed Gaussian-Lorentzian components using CasaXPS software. To compensate for surface charging effects in the insulating samples, all binding energies were corrected with reference to the saturated hydrocarbon C 1s peak at 285.0 eV using the CasaXPS software. In order to minimize the amount of ubiquitous carbonaceous contamination which proportionally increases with time, samples were individually loaded in the chamber.

Solid Phase Peptide Synthesis. The peptides KLPGWSG (K7), AFILPTG (A7) and LDHSLHS (L7) were prepared using a microwave-assisted solid phase peptide synthesizer (CEM Corporation) via Fmoc chemistry[13] as previously described.[6] The Mw of K7, A7 and L7, 743.4 g/mol, 717.8 g/mol and 807.4 g/mol, respectively; was confirmed with their measured m/z of 744.4 m/z, 718.4 m/z and 808.1 m/z, respectively (**Figure S1** in Supporting Information). **Table 1** details the physicochemical properties of the peptides, K7 (KLPGWSG), A7 (AFILPTG) and L7 (LDHSHS).

Table 1 Peptide properties

Peptide name	Peptide Sequence	pI	ξ[a]	Average Hydrophilicity[b] / Hydrophobicity[c]	Number of side-chain functionalities				
					Basic	acidic	Polar[d]	Non-polar[e]	hydroxyl
K7	KLPGWSG	10	+1	-0.3 / 18.7	1	0	3	3	1
A7	AFILPTG	6	0	-1.0 / 26.4	0	0	2	5	1
L7	LDHSLHS	6	-1	-0.1 / 10.7	2	1	2	2	2

[a]Net charge pH 7.4, [b]calculated from http://www.bachem.com/service-support/peptide-calculator/, [c]calculated from https://www.thermofisher.com/uk/.../peptides...peptide.../peptide-analyzing-tool.html, [d]uncharged and [e]hydrophobic.

Binding Studies. Silica particles were suspended (1 mg·ml^{-1}) in 10mM phosphate-buffered saline (pH = 7.4) and sonicated for 1 hour, followed by the addition of peptide solution of desired concentration and incubated for another hour. Langmuir adsorption isotherms have been reported when a protein approaches a solid interface;[5,14] however, previous studies in our group have shown that the adsorption isotherms of the peptides used in this study follow the Freundlich model, where saturation is achieved at values higher than 1.0 mM.[6] Thus, the peptide concentration range chosen for this study was from 0.1 - 1.0 mM. After 1 hour of mixing, samples were centrifuged at 13000 rpm for 5 minutes at 20 °C. For the assay, 180 µl of the supernatant was dispensed into a black 96-well plate. To this aliquot, 20 µl of fluorescamine solution (5 mg·ml^{-1} in acetone) was added and mixed (shaking for 60 seconds) immediately prior to measurement of the fluorescence intensity. The silica-peptide binding measurements were performed using fluorescence spectroscopy (TECAN i-control M200) on Corning® black polystyrene 96-well plates. The excitation wavelength was set at 360 nm and the emission (sample reading) was at 465 nm. The gain of the photomultiplier was adjusted to 60 a.u. for the best signal-noise.

Desorption Studies. Precipitates were washed with phosphate buffered saline and incubated for an hour at room temperature. Samples were then centrifuged at 13000 rpm for 5 minutes at room temperature. An aliquot of 60% of the volume was taken for analysis (following the methodology described above for measurement of peptide). This procedure was repeated 3 more times. Note, this study was carried out to prove strength of interaction. In this case, final concentrations of the peptides K7 and A7 were 0.25 mM and 1 mM, respectively.

Isothermal titration calorimetry Studies. ITC studies were conducted using a Malvern MicroCal VP instrument and data analysis conducted using ORIGIN 2018 software. For ITC measurements, peptides (K7) and SiNPs (non-functionalised and functionalised with 500 mM of APTES) were

dispersed in phosphate buffered saline at a pH of 7.4 to prepare 200 μM and 20 μM stock solutions, respectively. The system parameters were; cell temperature at 25 ˚C, reference power of 15 and 17 μcal·s^{-1} for non-functionalised and functionalised particles respectively. A stirring speed of 307 rpm was used to maintain SiNPs in suspension. The spacing between each injection in seconds was programmed to allow for equilibrium to be reached after each injection. Each experiment had a total duration of around 8.5 hours and was repeated at least in duplicate to ensure reliability of the results. For obtaining the values for K_a a linear fitting was used and enthalpy was taken from the amplitude of the dataset.

C**ircular dichroism studies.** For CD measurements, synthetic peptides (>95%, JPT, Germany) were dissolved in a 10 mM phosphate buffer solution at a pH of 7.4 to prepare 2 mM stock solutions. CD spectra of the solvated peptides were recorded on an Applied Photophysics Chirascan spectrometer running the Pro-Data Chirascan software (v4.2.22). Three repeat scans for each sample were measured at 25 °C over the wavelength range 250 to 180 nm using an interval of 1 nm in Suprasil quartz cells (Hellma UK Ltd.) with a pathlength of 0.01 cm. For each of the triplicate measurements the baselines were subtracted and the net spectrum smoothed with a Savitsky-Golay Filter using a smoothing window of 5 data points. The mean residue ellipticity θ_{MRE} was calculated using:[15]

$$\theta_{MRE} = \frac{\theta_{mdeg}}{c \cdot l \cdot n} \quad [1]$$

where θ_{mdeg} is the raw measured CD signal in mdeg, n corresponds to the number of amino acids, l is the pathlength of the quartz cuvette and c the molar concentration of the peptide. Peptide concentrations were determined using UV absorbance at 205 and 214 nm.[16,17] Analysis of the measured CD spectra regarding the secondary structural components has been performed via the

BeStSel webserver.[18] To measure the adsorbed peptides on the different SiNPs surfaces, peptide stock solutions (2 mM) were mixed with silica particles (28nm particles at 2 $mg \cdot ml^{-1}$) and incubated for 1 hour in an overhead shaker. Samples were then centrifuged at 13000 rpm for 10 minutes at 20 °C, the supernatant removed completely (250 µl) and the pellet immediately (prior to the CD measurement) resuspended in 250 µl phosphate buffer solution. Three CD measurements were completed within less than 5 minutes to ensure measurement spectra from absorbed peptide. Analysis of the spectra was performed as for the solvated peptides. Due to their lack of stability in suspension no CD experiments could be performed on the larger (210 nm diameter) silica nanoparticles.

Results and discussion

Silica Particle Properties and Levels of Functionalization Achieved. Characterization of the silica particles and peptides used a range of experimental techniques and is provided in the Supporting Information (**S1-S5**). In short, silica particle sizes of 28 and 210 nm were synthesized and functionalized with varying levels of methyl and amino groups. Zeta potential measurements, **Table 2**, TGA data (S5) and XPS data (S6) of the samples provided direct evidence for the level of functionalization.

Table 2 Zeta potential values (mV) for SiNPs of different size and functionalities (pH 7.4 ± 0.1).

ξ (mV) pH 7.4	***$[X]_{added}$ (mM)***	***28-SiO_2***	***210-SiO_2***
OH-SiO_2	---	-18.3 ± 0.6	-33.3 ± 3.6
CH_3-SiO_2	10	-17.3 ± 1.6	-28.0 ± 1.1
	500	-14.9 ± 0.2	-22.3 ± 2.1
NH_2-$(CH_2)_3$-SiO_2	10	-13.1 ± 0.6	-17.8 ± 1.2
	500	+9.1 ± 1.8	+2.2 ± 0.4

For non-functionalized silica samples, XPS spectra (in supporting Information **S6**) showed the characteristic peaks of Si 2p and O 1s, at 103 eV and 532 eV, respectively; as well as the incorporation of C and/or N by detection of peaks in the region of C 1s (285 eV) and N 1s (399 eV). The atomic % of Si, O, C and N for the different silica sizes studied are shown in **S6** in the Supporting Information. Note that XPS is a solid-state surface characterization technique that requires high vacuum for data collection. As such it is only able to give an indication of the likely surface chemistry in solution. The technique was employed to validate the presence of MTEOS/APTES bound to the surface of the silica particles. The small amount of C detected in the pristine SiNPs was attributed to adventitious C present in the XPS chamber during analysis. In general, the area of the heteroatom C 1s and N 1s peaks increased with extent of functionalization (**Table S6**). The extent of methyl and 3-aminopropyl functionalization for the different particle sizes was studied by comparing the ratio of C:Si and N:Si on the silica surface, respectively (**Figure 1a-b**).

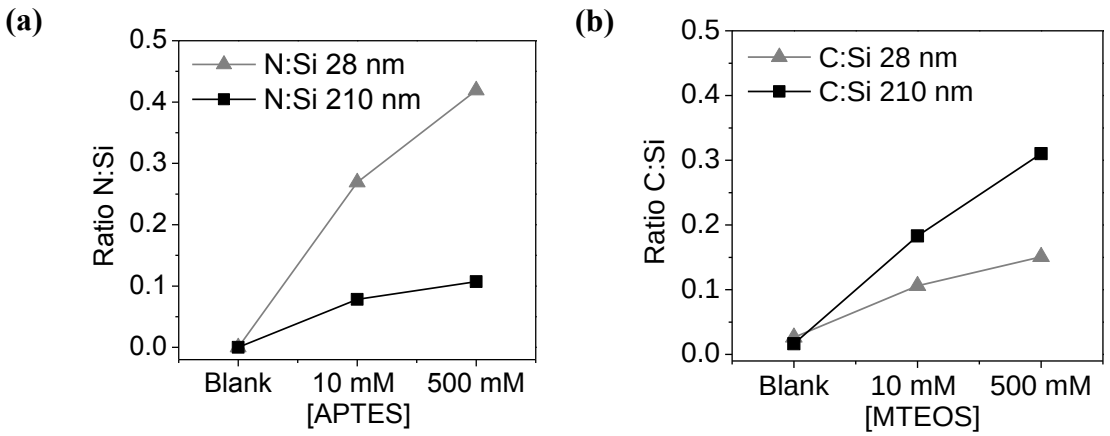

Figure 1 (a) N:Si ratio and (b) C:Si ratio on the silica particles showing trend of functionalization vs. particle size. Note lines are to guide the eye only.

For the 3-aminopropyl surfaces, a higher % of N for the smaller particles (~8%) compared with the bigger particles (~3%) was detected. From the surface charge values, **Table 2**, it would be expected that the more negative the charge, the more amino groups would be attracted to the surface; however, our results show that the higher surface area of the particles (**S3**), the more 3-aminopropyl groups could be attached to the surface. The data suggest that independent of the particle charge, amino groups attach preferentially to smaller silica particles. For the 210-SiO_2 NPs, an increase of N % was detected as the concentration of APTES added into the system was increased, indicating that coverage was probably below a monolayer as previously reported.[8] For the 28-SiO_2 NPs, the % of atomic N also showed an increase with the different levels of APTES used and further showed a different distribution of NH_3^+ and NH_2, **SI 6** shows deconvolution of the N 1s band (from core-level spectra) from XPS analysis. The net positive zeta potential charge (**Table 2**) and the increased % weight loss (TGA data **S5**) for the higher concentration of APTES used, suggested that the original silica particles were coated in a much thicker layer of silica incorporating amino groups as well as the coating being able to more efficiently mask the original negative silica charge. We believe that x-ray penetration was sufficient to see amine groups exposed at the outer surface layer but not all amine groups attached to the silica particles. Further, there are many different ways in which APTES can interact with a silica surface according to the existing functionality.[19] Protonated amine groups can either adsorb on the silica surface (negatively charged) via electrostatic interactions (**Figure 2a**) or through the ethoxy moieties via covalent interactions, **Figure 2b**, exposing free amines on the outer surface layer. Note that, the free amines can also exist as protonated groups and the ethoxy groups are more likely to be hydrolysed due to the experimental working pH of 7.4. Further, the free amines can also interact with ionised silanol groups on the surface (**Figure 2c**). Other weaker interactions, such as hydrogen bonding between

amine groups and surface hydroxyls could also occur (**Figure 2d**). In addition, further condensation of additional APTES molecules with any APTES molecules bound via interactions such as in (a), (c) or (d) will also lead to a thicker surface layer. Therefore, depending on the orientation of APTES on the silica surface, the species exposed to the outer functionalised silica layer will differ (i.e. free amine or silane groups) giving the surface a more hydrophilic character (i.e. free amines or hydrolysed ethoxy groups) or more hydrophobic character (i.e. propyl groups) which will be crucial for the mechanism of peptide binding that can take place.

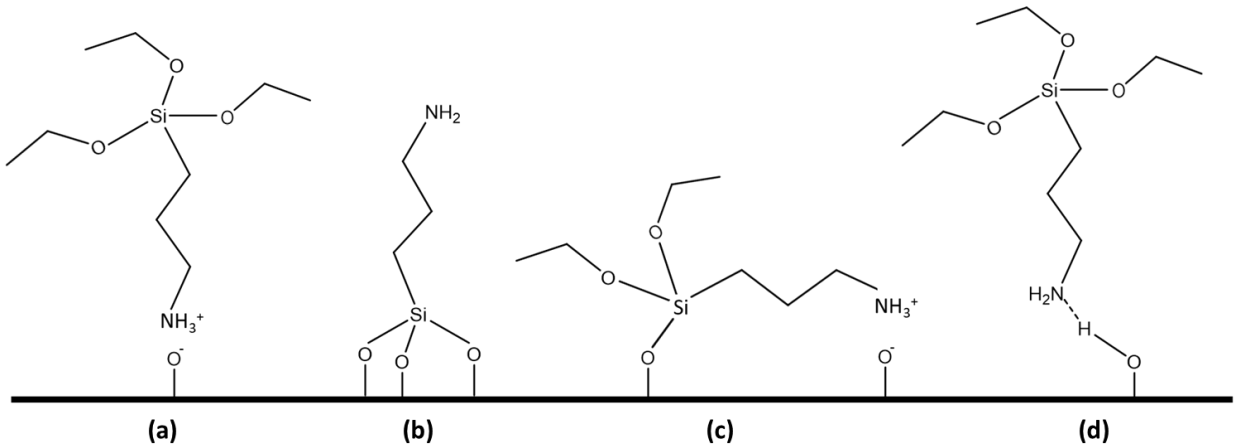

Figure 2 Schematic representation of possible orientations of APTES on the silica surface. Note- under the conditions used in the binding experiments it is likely that ethoxy groups are hydrolysed (and available for further condensation) and amine groups protonated.

For methyl functionalized surfaces, an increase of the ratio of C:Si with addition of higher amounts of MTEOS into the system was observed for both the 28-SiO_2 NPs and 210-SiO_2 NPs (**Figure 1b**), with the maximum % of C detected ~ 5% and ~10%, respectively. In this case, a higher extent of functionalization was achieved for larger SiNPs. This was in accordance with previous results, where 500 nm SiNPs showed ~19% of C (without inclusion of adventitious C the value is ~15%).[20] Further, the presence of a lower % of O in larger particles (XPS analysis of non-functionalized SiO_2 NPs, **S6**) suggested lower levels of silanol groups on the surface; and thus, a higher

hydrophobicity of the silica particles is expected due to the presence of more Si-O-Si linkages on the surface.

Silica-Peptide Binding Studies. Although the adsorption process highly depends on the nature/chemistry of the solid surface, other factors such as binding/kinetic energies and/or orientation/conformation of the peptide also play an important role on peptide adsorption.[5,14,21] The mechanism of protein or peptide binding has been shown to be a complex process involving electrostatic, hydrophobic, van der Waals interactions, and hydrogen bonding.[5-7,14] In **Table 1** are shown the properties of the peptides chosen for this study, K7 (KLPGWSG), A7 (AFILPTG) and L7 (LDHSHS), which are believed to affect the type of interactions taking place at the silica-aqueous interface. **Figure 3** shows their conformational ensemble behavior in solution as accessed by circular dichroism spectroscopy.

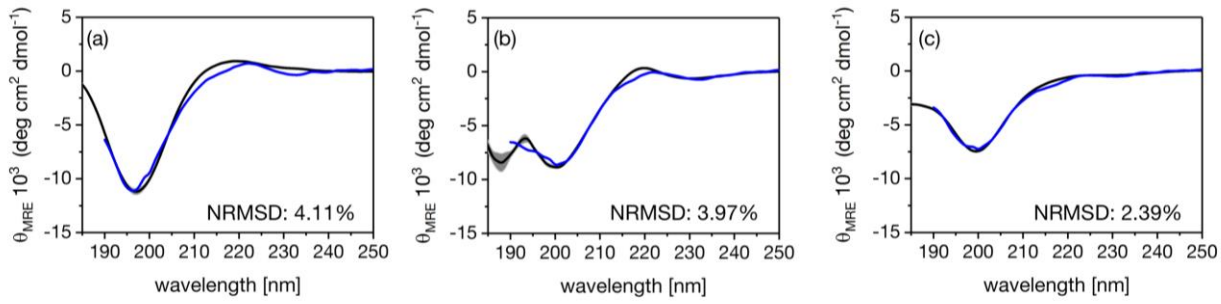

Figure 3 CD spectra in solution from (a) peptide K7; (b) peptide A7 and (c) peptide L7. The black lines show the averaged CD spectra from the triplicate measurements, the grey pattern reveals the deviation between the three measurements. The blue spectra are calculated from the BeStSel server during estimation of the secondary structure components. The NRMSD value given for each of the peptides describes the deviation between the predicted spectra and the average spectra calculated via the approach described in Misconai et al.[18]

Analysis of the conformational ensemble of all three binding peptides shows that they are largely unordered structures. Conformational instability is a common feature of bio-molecules involved in the recognition and binding to solid materials.[22] The inherent binding affinity of peptides is determined by the amino acid sequence and the secondary structure, which are believed to be a driving force for peptide mediated crystal growth and regulation. Unordered conformationally labile peptides enhance their adaptability of interfacial features at surfaces and lead to creation of accessible side chain regimes (Hnilova *et al*. 2008).[22] Besides the contribution of unordered conformations, the next most significant component arises from antiparallel beta strand structures. The three peptides differ in the ratio of these features (**S8-S10**) with the net positively charged peptide, K7 possessing the highest amount of beta strand content (> 40%), the overall neutral peptide A7 exhibiting the least amount of beta strand content (< 30%) and the net negatively charged peptide, L7 features < 40% antiparallel beta strand structures according to BeStSel. The secondary structure analysis of these peptides contained contributions from multiple beta strand spectral signatures (right-twisted antiparallel, relaxed antiparallel and left-twisted antiparallel beta strand) introduced from Micsonai *et al.*[18]

In comparison of the BeStSel and DichroWeb results (**S8 - S11**) regarding the deviation from the experimental spectra, BeStSel shows a significantly lower deviation. We believe this is due to the extended set of basis spectra included in BeStSel, with special emphasis of the description for beta-strand structures. These descriptions in BeStSel, but also from other approaches (DichroWeb and Brahms&Brahms),[23-27] have been usually developed based on much larger polypeptides and the transfer to small peptides needs to be done carefully since, with the exception of beta-hairpins, the definition of a twist is based on the presence of a second peptide and its orientation. In experimental

conditions the three peptides investigated in this work tend to form agglomerates[14] and might therefore orientate in an antiparallel or parallel manner.

Previous experimental and computational studies have shown that silica peptide interactions are peptide and particle size dependent[6,8,9] and correlation between surface charge and particle size can be used as a proxy to compare the binding of peptides to silica particles of different size. In this study, it was possible to measure peptides bound to 28 nm silica particles using CD spectroscopy. For all three peptides, the experimentally derived spectra for peptide adsorbed on the pristine 28 nm silica nanoparticles do not differ significantly from that measured for the peptide alone in terms of the minimum position and intensity, indicating that the adsorption process does not have a strong influence on the conformational ensemble of the bound peptides. Slight changes can only be observed in the wavelength region below 195 nm. Changes within this wavelength region could be associated with changes in the $\pi \rightarrow \pi^*$ transitions along the C=O bond of the peptide backbone, which are also sensitive to adjacent bonding in close proximity to the chromophore.[15] However, this wavelength region is also sensitive to increasing adsorption contributions from the solvent, nanoparticles as well as the peptide itself.

The effect of extent of -methyl and -amino functionalization on peptide binding for both small (28 nm) and large (210 nm) silica particles was also studied; with CD data being generated for the small particles only owing to issues with particle sedimentation as described in the materials and methods section. The tables containing the secondary analysis of the experimental CD spectra via BeStSel[18]are shown in supporting information (**S8-S10**).

As for prior experimental studies (by Puddu and Perry (2014))[8] a higher peptide affinity for larger particles was observed independent of the peptide identity and peptide affinity increased generally

from L7 < A7 < K7 (**S7**). The effect of functionalization on peptide binding was functional group and particle size dependent with the most significant effects being observed for the amino functionalized silica particles.

The extent of amino functionalization on silica particle surfaces significantly affected peptide affinity (**Figure 4**). For K7 (**Figure 4a**), peptide affinity decreased with functionalization, Si-OH > NH_2-$(CH_2)_3$-SiO_2, when only low levels (10 mM) of APTES was added to the system. However, when surface functionalization was increased (500 mM APTES), higher interaction compared with the pristine SiO_2 was observed for both particle sizes studied; the effect being greatest for the smaller positively charged particles (**Figure 4ai**), where higher levels of amino functionalization had been measured by XPS (**Table in S6**). This was manifested in the CD spectral data only by differences in the intensity depending on the extent of the functionalization. Though changes in the proportions of secondary structural components were slight, they could be attributed to β-strand composition especially the contribution of relaxed antiparallel and right-twisted antiparallel β-strands.[18] This behavior could be correlated with a change in measured zeta potential for the 28 and 210 nm SiNPs; ~9 and ~2 mV, respectively (**Table 2**). For peptide A7 (**Figure 4b**), similar behavior on binding was observed for the highest level of amine functionalization (500 mM) for the smallest particles, even though this peptide has been shown to interact largely by hydrogen bond/ hydrophobic interactions, thus, lower affinity towards the 3-aminopropyl-SiO_2 could be expected.[8] The CD results for the adsorbed spectra showed a slight difference in the wavelength region below 195 nm in comparison to the spectra associated with the conformational ensemble in solution (**Figure 3biii**). However, according to the analysis of the structural compositions, the obtained difference was not significant and independent of the extent of functionalization and led to a conformational ensemble very similar for both functionalization systems, MTEOS and APTES

(Supporting information **S8-S10**). For peptide L7 (**Figure 4c**), a higher interaction with the 3-amino-propyl surfaces compared to pristine silica was observed due to electrostatic interactions as previously reported.[8] Levels of amino functionalization affected peptide adsorption for the smallest particle size. Although more interaction would have been expected for higher levels of amine groups on the surface (positively charged surfaces), adsorption isotherms showed the opposite trend, being very significant for the SiO_2-28 nm particles. It should be noted that for smaller particles (28 nm), significant differences of L7 uptake between amino functionalized surfaces and pristine silica was observed at very low initial concentrations whereas for larger particles a threshold concentration was required to observe such differences. In support, the CD spectra reveal a difference between solvated and the adsorbed spectra for pristine as well as functionalized nanoparticles, independent of the kind and the amount of functionalization, and show a slight increase of β-strand content (and hence order) upon adsorption.

Similar measurements conducted on methyl functionalized materials by both fluorimetry and CD analysis (**Supporting Information S11**) showed much smaller differences in binding behavior suggesting little effect of the methyl functional levels on peptide binding.

The adsorption isotherms in **Figure 4** agree with previous findings where peptide binding response is significantly affected by small changes on the silica surface such as low degree of functionality.[20] However, these results also provide evidence of a different peptide response towards silica surfaces containing higher amounts of amine groups. **Scheme 1** depicts possible binding mechanisms occurring at the aqueous silica interface with different levels of amine-functionalization.

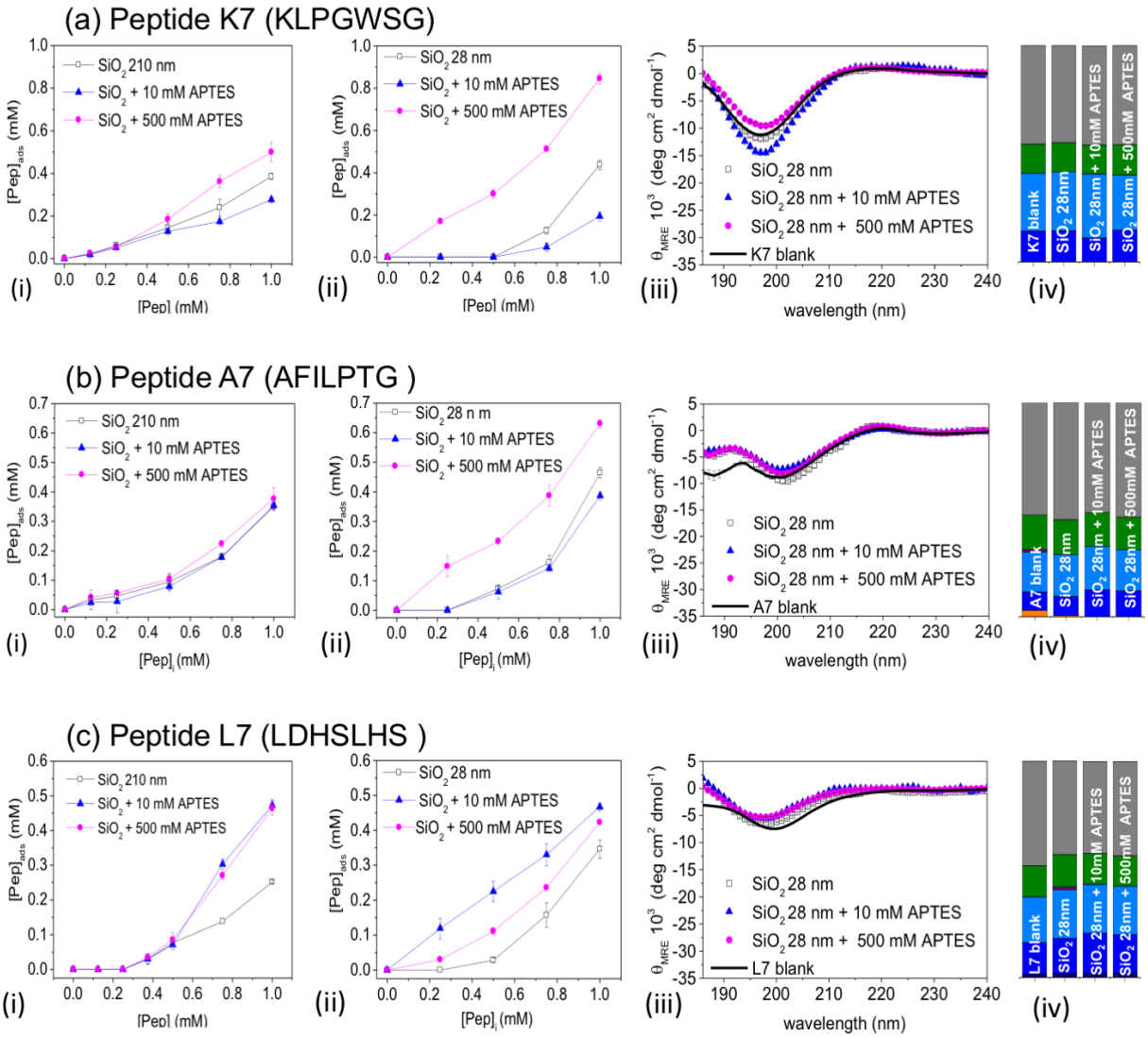

Figure 4 Adsorption isotherms of the peptides (a) K7 (KLPGWSG), (b) A7 (AFILPTG) and (c) L7 (LDHSLHS) on amine-functionalized SiNPs of different size; (i) 210 nm and (ii) 28 nm; with (iii) the corresponding CD spectra and (iv) their structural analysis via BeStSel.

Interaction strength was also investigated by ITC where the thermodynamic properties of these interactions can be directly evaluated and the association constant (K_A) of the system determined. The K_A of peptide K7 (as a representative) to APTES functionalized, positively charged 28 nm

diameter silica was ca. five times higher ($1.56 \times 10^4 \pm 3.3 \times 10^3$ M^{-1}) than to the unfunctionalized, negatively charged particles ($3.05 \times 10^3 \pm 3.7 \times 10^2$ M^{-1}). These values were in agreement with our findings from the absorption studies discussed above (**Figure 4a**). ITC also allowed for the direct determination of enthalpy (ΔH), entropy (ΔS) and Gibbs free energy (ΔG) for binding events in solution (**Table 3)**. Little difference in ΔS between the two sets of particles suggested little difference in reorganization energy on the different surfaces though the CD data did suggest a change in the conformational ensemble. The values of delta ΔH and ΔG are suggestive of an enthalpically driven binding process which is more energetically favoured for the amine functionalized surface.

Table 3 Thermodynamic parameters; ΔH, ΔS and ΔG obtained by ITC measurement of the interaction of peptide K7 with non-functionalized and positively charged APTES (500 mM) functionalized SiNPs.

System **28-SiO_2 + K7**	**K_A (M^{-1})**	**K_D (M^{-1})**	**ΔH ($KJmol^{-1}$)**	**ΔS ($JK^{-1}mol^{-1}$)**	**ΔG ($KJmol^{-1}$)**
SiO_2	$3.05x10^3 \pm 368$	332.0 ± 40.1	-3.3 ± 0.5	55.6 ± 2.7	-19.9 ± 1.3
APTES-SiO_2	$1.56x10^4 \pm 3319$	71.2 ± 13.3	-8.4 ± 0.2	51.6 ± 2.2	-23.8 ± 0.8

In order to understand the possible binding mechanism(s) taking place at the silica aqueous interface, desorption studies were conducted (**Figure 5**). The results showed that significant levels of peptide A7 (and K7) remain attached to positively charged APTES functionalized silica particles (after extensive washing), suggesting that binding of these peptides to silica, although for some molecules involves electrostatic and 'weaker' i.e. van der Waals/ hydrogen bonding interactions, there are additional 'strong' interactions that prevent the peptide from being removed from the silica. We suggest these might be extensive hydrophobic interactions caused by the peptides containing large numbers of non-polar residues, with a higher contribution of such

interactions exist for the peptide A7 than for peptide K7, **Table 1**. These results would also be in agreement with our surface characterization studies where different orientations of APTES onto the silica surface were suggested (**Figure 2**).

In addition, although it is difficult to prove the presence of covalent interactions from the experimental data obtained, the possibility should not be discarded. One possibility would involve attack of an hydroxyl group present in a peptide (Ser or Thr) on any remaining ethoxy groups from APTES already interacting with the surface leading to the formation of further Si-O-C bonds. This might be favourable if the peptide is associated with the surface of the particles via extensive hydrophobic interactions, a situation which is possible for both the K7 and A7 peptide in the presence of the positively charged APTES functionalized particles.

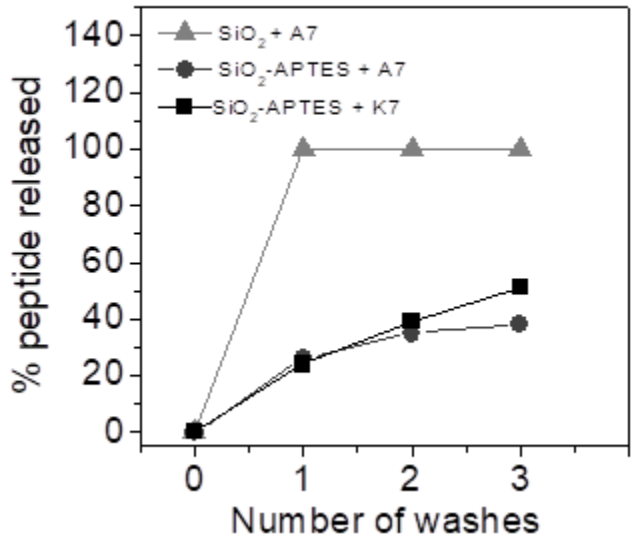

Figure 5 Peptide released (%) from silica or APTES treated silica during desorption studies.

We return now to consider how the peptides studied interact with the surfaces of the (un) functionalized silica particles. For K7 peptide (positively charged peptide), electrostatic interactions, probably via the N-terminus and lysine dominate for pristine silica (negatively charged surface). As the charge on the particle surface is decreased (low level of functionalization) the amount of peptide bound similarly decreases, as could be anticipated assuming these are the main contributions to binding. For A7, the desorption data confirm that binding to negatively charged particles is dominated by electrostatic interactions, though probably with some contribution from other weaker interactions too. For both K7 and A7, the increase of peptide affinity with increased amino functionalization (positively charged particle surfaces) suggest electrostatic interaction via the C-terminus and other 'strong' interactions other than electrostatic occur at the silica aqueous interface. Both peptides have considerable hydrophobic character, **Table 1** with amino acids such as Pro, Ile, Leu, Phe and Trp able to contribute to hydrophobic interactions, as previously reported.[8] In addition, the potential formation of covalent interactions between unreacted ethoxy groups and the hydroxyl groups of Ser and Thr cannot be totally discounted. The switch of peptide binding mechanism found for these positively charged amino functionalized surfaces can be of great interest for biomedical applications[2] but also for industrial purposes since hydrophobic materials, such as polymers or (slightly) hydrophobic silica nanoparticles, have been shown to be more efficient in oil recovery in low permeability sandstone reservoirs.[28,29]

For L7, which is a much more hydrophilic peptide is, **Table 1**, we do not see the same binding behavior for the amine functionalized SiNPs. The results indicate that for high levels of amino-functionalized surfaces this peptide might interact via the basic amino residues (i.e. histidine) instead of the overall charge of the peptide under the experimental conditions used. The 'switch'

of peptide adsorption behavior towards the highly amino-functionalized surface observed for these SiNPs suggests that the peptide binding mechanism, in this case, may involve the C-terminus (-COOH group) of the peptide and the surface -NH_3^+ groups, involving acid/base interactions. For the methyl-functionalized surfaces, the peptide affinity did not change significantly according to the extent of surface functionalization with the results obtained being compatible with prior studies.[8,9] In **Scheme 1** are proposed the governing interactions at the silica aqueous interface for the different functionalised SiNPs.

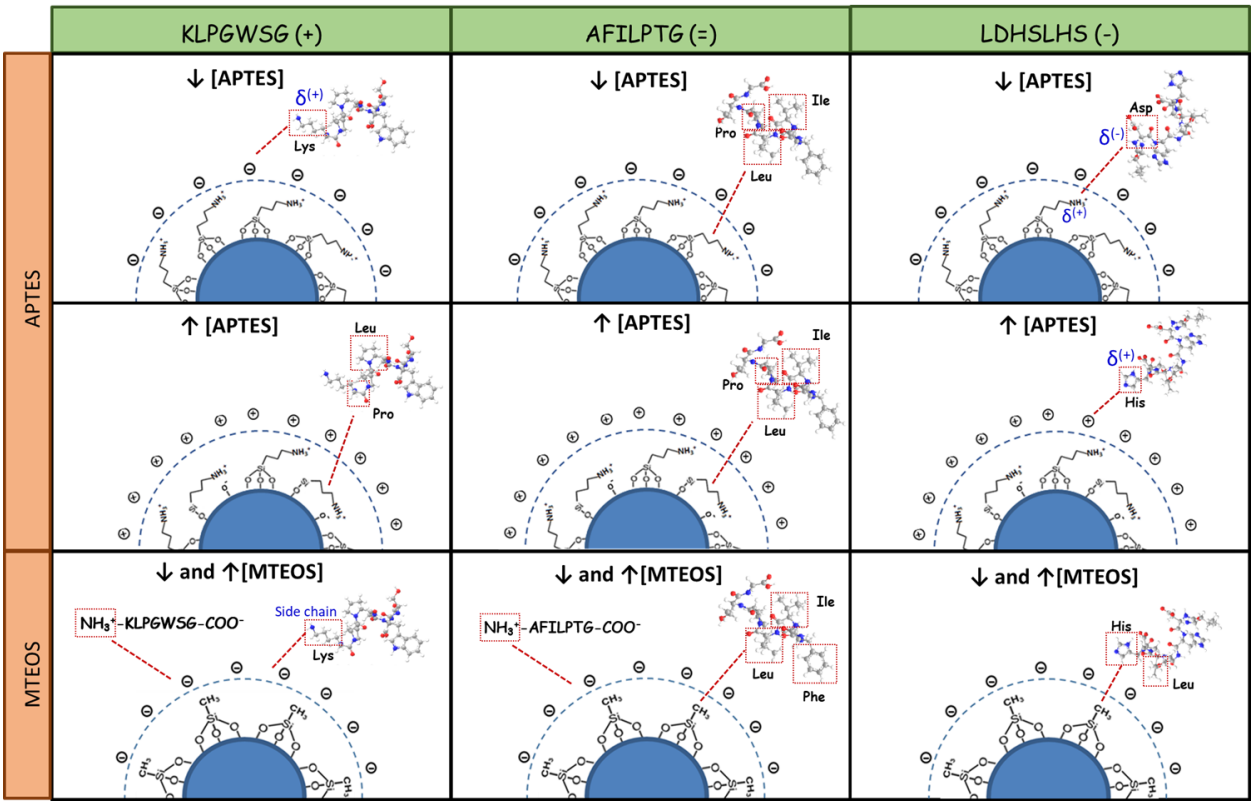

Scheme 1 Possible binding mechanisms occurring at the silica aqueous interface.

Conclusions

From this investigation, the extent of silica functionalization was key to determining peptide affinity/ binding characteristics and further, the study highlights the need to understand the precise

chemistry and topography of the solid surface under study to comprehend their effect on peptide adsorption. Although, different levels of surface functionalization were attained by APTES or MTEOS addition; the level of surface functionalization was shown to be particle-size dependent due to different chemistry properties (i.e. surface area, porosity, charge) of 28 and 210 nm SiNPs. Our results showed that when using the same concentration of functional groups, a higher amount of 3-aminopropyl functionality can be achieved for smaller particles, while a higher degree of methyl groups is more likely to be found on larger particles implying significant differences on the surface properties (i.e. net charge) for the different particle sizes. As peptide binding response depends on the nature/chemistry of the solid surface, significant differences were observed at the silica-peptide interface by the surface functionalities and the extent of functionalization (remarkably for amine-functionalized surfaces) where a 'switch' of peptide adsorption behavior was demonstrated at increasing levels of functionalization on the silica surface. Using a combination of data from isothermal titration calorimetry and peptide desorption studies we were able to show a higher affinity of peptides K7 and A7 towards the positively charged amino functionalized surface and confirm the presence of binding modes other than electrostatic interactions contributing to the binding mechanism. CD spectroscopy used to assess the sensitivity of the conformational ensemble to the adsorption process was able to show that for peptides A7 and L7, although the amount of adsorption for these two peptides can be influenced via the chemical identity and extent of functionalization, the conformational ensemble is only influenced by the adsorption process itself. In contrast the conformational ensemble of the peptide K7 is not influenced by the adsorption on pristine and MTEOS functionalized silica nanoparticles but is sensitive to the extent of functionalization for the amino functionalized SiNPs.

ASSOCIATED CONTENT

Supporting Information. Figures and tables. This material is available free of charge via the Internet at http://pubs.acs.org.

Corresponding Author

* E-mail: Carole.Perry@ntu.ac.uk.

Author Contributions

The manuscript was written through contributions of all authors. All authors have given approval to the final version of the manuscript.

Funding Sources

We are very grateful to the U.S. Air Force Office of Scientific Research (AFOSR) for funding (FA9550-16-1-0213 and FA9550-13-1-0040).

ACKNOWLEDGMENT

The authors are grateful to D.J. Belton for his knowledge in this field, G. Hickman for mass spectrometry analysis and Ben Hanby for XPS support. The authors are grateful to Jonathan Hirst and József Kardos for fruitful discussions regarding the measurement and calculation of CD spectra.

ABBREVIATIONS

SiNPs, silica nanoparticles; K7, 7-mer peptide starting with amino acid Lysine; A7, 7-mer peptide starting with amino acid Alanine; L7, 7-mer peptide starting with amino acid Leucine; CD, circular dichroism.

References

1. Sanchez, C.; Arribart, H.; Guille, M. M. G. Biomimetism and bioinspiration as tools for the design of innovative materials and systems. *Nature materials* **2005***, 4*, 277-288.

2. De Jong, W. H.; Borm, P. J. Drug delivery and nanoparticles:applications and hazards. *Int. J. Nanomedicine* **2008***, 3*, 133-149.

3. Zou, H.; Wu, S.; Shen, J. Polymer/silica nanocomposites: preparation, characterization, properties, and applications. *Chem. Rev.* **2008***, 108*, 3893-3957.

4. Knopp, D.; Tang, D.; Niessner, R. Review: bioanalytical applications of biomolecule-functionalized nanometer-sized doped silica particles. *Anal. Chim. Acta* **2009***, 647*, 14-30.

5. Roach, P.; Farrar, D.; Perry, C. C. Interpretation of protein adsorption: surface-induced conformational changes. *J. Am. Chem. Soc.* **2005***, 127*, 8168-8173.

6. Puddu, V.; Perry, C. C. Peptide adsorption on silica nanoparticles: Evidence of hydrophobic interactions. *ACS Nano* **2012***, 6*, 6356-6363.

7. Patwardhan, S. V.; Emami, F. S.; Berry, R. J.; Jones, S. E.; Naik, R. R.; Deschaume, O.; Heinz, H.; Perry, C. C. Chemistry of aqueous silica nanoparticle surfaces and the mechanism of selective peptide adsorption. *J. Am. Chem. Soc.* **2012***, 134*, 6244-6256.

8. Puddu, V.; Perry, C. C. Interactions at the Silica-Peptide Interface: The Influence of Particle Size and the Surface Functionality. *Langmuir* **2014***, 30*, 227-233.

9. Emami, F. S.; Puddu, V.; Berry, R. J.; Varshney, V.; Patwardhan, S. V.; Perry, C. C.; Heinz, H. Prediction of Specific Biomolecule Adsorption on Silica Surfaces as a Function of pH and Particle Size. *Chem. Mater.* **2014***, 26*, 5725-5734.

10. Stöber, W.; Fink, A.; Bohn, E. Controlled growth of monodisperse silica spheres in the micron size range. *J. Colloid Interface Sci.* **1968***, 26*, 62-69.

11. Brunauer, S.; Emmett, P. H.; Teller, E. Adsorption of gases in multimolecular layers. *J. Am. Chem. Soc.* **1938***, 60*, 309-319.

12. Barrett, E. P.; Joyner, L. G.; Halenda, P. P. The determination of pore volume and area distributions in porous substances. I. Computations from nitrogen isotherms. *J. Am. Chem. Soc.* **1951***, 73*, 373-380.

13. Chan, W.; White, P., Eds.; In *Fmoc Solid Phase Peptide Synthesis: A Practical Approach;* Oxford University Press: New York, 2000; .

14. Rabe, M.; Verdes, D.; Seeger, S. Understanding protein adsorption phenomena at solid surfaces. *Adv. Colloid Interface Sci.* **2011***, 162*, 87-106.

15. Greenfield, N. J. Using circular dichroism spectra to estimate protein secondary structure. *Nature protocols* **2006***, 1*, 2876-2890.

16. Anthis, N. J.; Clore, G. M. Sequence- specific determination of protein and peptide concentrations by absorbance at 205 nm. *Protein Science* **2013***, 22*, 851-858.

17. Kuipers, B. J.; Gruppen, H. Prediction of molar extinction coefficients of proteins and peptides using UV absorption of the constituent amino acids at 214 nm to enable quantitative reverse phase high-performance liquid chromatography-mass spectrometry analysis. *J. Agric. Food Chem.* **2007***, 55*, 5445-5451.

18. Micsonai, A.; Wien, F.; Kernya, L.; Lee, Y. H.; Goto, Y.; Refregiers, M.; Kardos, J. Accurate secondary structure prediction and fold recognition for circular dichroism spectroscopy. *Proc. Natl. Acad. Sci. U. S. A.* **2015***, 112*, E3095-103.

19. Asenath Smith, E.; Chen, W. How to prevent the loss of surface functionality derived from aminosilanes. *Langmuir* **2008***, 24*, 12405-12409.

20. Ek, S.; Root, A.; Peussa, M.; Niinistö, L. Determination of the hydroxyl group content in silica by thermogravimetry and a comparison with 1H MAS NMR results. *Thermochimica acta* **2001***, 379*, 201-212.

21. Gray, J. J. The interaction of proteins with solid surfaces. *Curr. Opin. Struct. Biol.* **2004***, 14*, 110-115.

22. Hnilova, M.; So, C. R.; Oren, E. E.; Wilson, B. R.; Kacar, T.; Tamerler, C.; Sarikaya, M. Peptide-directed co-assembly of nanoprobes on multimaterial patterned solid surfaces. *Soft Matter* **2012***, 8*, 4327-4334.

23. Whitmore, L.; Wallace, B. DICHROWEB, an online server for protein secondary structure analyses from circular dichroism spectroscopic data. *Nucleic Acids Res.* **2004***, 32*, W668-W673.

24. Whitmore, L.; Wallace, B. A. Protein secondary structure analyses from circular dichroism spectroscopy: methods and reference databases. *Biopolymers* **2008***, 89*, 392-400.

25. Lees, J. G.; Miles, A. J.; Wien, F.; Wallace, B. A reference database for circular dichroism spectroscopy covering fold and secondary structure space. *Bioinformatics* **2006***, 22*, 1955-1962.

26. Provencher, S. W.; Gloeckner, J. Estimation of globular protein secondary structure from circular dichroism. *Biochemistry (N. Y.)* **1981***, 20*, 33-37.

27. Brahms, S.; Brahms, J. Determination of protein secondary structure in solution by vacuum ultraviolet circular dichroism. *J. Mol. Biol.* **1980***, 138*, 149-178.

28. Zargartalebi, M.; Kharrat, R.; Barati, N. Enhancement of surfactant flooding performance by the use of silica nanoparticles. *Fuel* **2015***, 143*, 21-27.

29. Taylor, K. C.; Nasr-El-Din, H. A. Water-soluble hydrophobically associating polymers for improved oil recovery: A literature review. *Journal of Petroleum Science and Engineering* **1998***, 19*, 265-280.